Superfluid Quenching of the Moment of Inertia in a Strongly Interacting Fermi Gas

S. Riedl,[1,2] E. R. Sánchez Guajardo,[1,2] C. Kohstall,[1,2] J. Hecker Denschlag,[1,*] and R. Grimm[1,2]

[1] *Institut für Experimentalphysik and Zentrum für Quantenphysik, Universität Innsbruck, 6020 Innsbruck, Austria*
[2] *Institut für Quantenoptik und Quanteninformation, Österreichische Akademie der Wissenschaften, 6020 Innsbruck, Austria*

(Dated: July 22, 2009)

We report on the observation of a quenched moment of inertia as resulting from superfluidity in a strongly interacting Fermi gas. Our method is based on setting the hydrodynamic gas in slow rotation and determining its moment of inertia by detecting the precession of a radial quadrupole excitation. The measurements distinguish between the superfluid or collisional origin of hydrodynamic behavior, and show the phase transition.

PACS numbers: 67.85.Lm, 67.25.dg, 05.30.Fk, 34.50.Cx

Superfluidity is a striking property of quantum fluids at very low temperatures. For bosonic systems, important examples are liquids and clusters of ^{4}He and atomic Bose-Einstein condensates. In fermionic systems, superfluidity is a more intricate phenomenon as it requires pairing of particles. Fermionic superfluidity is known to occur in atomic nuclei and ^{3}He liquids and it is also at the heart of superconductivity, thus being of great technological importance. Recent advances with ultracold Fermi gases have opened up unprecedented possibilities to study the properties of strongly interacting fermionic superfluids [1, 2]. Early experiments on ultracold Fermi gases with resonant interparticle interactions compiled increasing evidence for superfluidity [3, 4, 5, 6, 7, 8] until the phenomenon was firmly established by the observation of vortex lattices [9].

In this Letter, we report on the manifestation of superfluidity in a quenched moment of inertia (MOI) in a strongly interacting Fermi gas undergoing slow rotation. The basic idea of a quenched MOI as a signature of superfluidity goes back more than 50 years in nuclear physics, where MOIs below the classical, rigid-body value were attributed to superfluidity [10]. The quenching of the MOI was also shown in liquid ^{4}He [11] and has, more recently, served for the discovery of a supersolid phase [12]. Here we introduce the observation of the quenched MOI as a new method to study superfluidity in ultracold Fermi gases.

Our basic experimental situation is illustrated in Fig. 1. At a finite temperature below the critical temperature T_c, the harmonically trapped cloud consists of a superfluid core centered in a collisionally hydrodynamic cloud. We assume that the trapping potential is close to cylindrical symmetry, but with a slight, controllable deformation that rotates around the corresponding axis with an angular velocity $\Omega_{\rm trap}$. The nonsuperfluid part of the cloud is then subject to friction with the trap and follows its rotation with an angular velocity Ω, which in a steady state ideally reaches $\Omega = \Omega_{\rm trap}$. The corresponding angular momentum can be expressed as $L = \Theta\Omega$, where Θ denotes the MOI. The superfluid core cannot carry angular momentum, assuming that vortex nucleation is avoided, and does therefore not contribute to the MOI of the system. Thus Θ represents the effective MOI of the whole system.

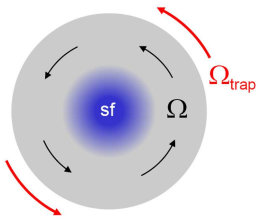

Figure 1: Schematic illustration of a strongly interacting Fermi gas in a slowly rotating trap. The normal part in the outer trap region rotates with a frequency Ω, which in an equilibrium state corresponds to the rotation frequency $\Omega_{\rm trap}$ imposed by the trap. The superfluid does not carry angular momentum and does therefore not contribute to the MOI.

The case of a rotating system in a steady state, where the normal part carries the maximum possible angular momentum, allows us to distinguish the superfluid quenching of the MOI from another effect studied in Ref. [13]. The latter originates from irrotational flow and may also be discussed in terms of a MOI below the rigid-body value, but it can occur for both the superfluid and the collisionally hydrodynamic normal phase.

Our measurements rely on the possibility to determine the total angular momentum L of a rotating hydrodynamic cloud by detecting the precession of a radial quadrupole excitation. This method is well established and has been extensively used in the context of atomic Bose-Einstein condensates [14, 15, 16] and recently also with strongly interacting Fermi gases [17]. The precession frequency can be written as $\Omega_{\rm prec} = L/(2\Theta_{\rm rig})$ [18], where $\Theta_{\rm rig}$ corresponds to a moment of inertia as calculated from the density distribution under the assumption that the whole cloud, including the superfluid part, would perform a rigid rotation. Substituting $\Theta\Omega$ for L, we obtain $\Omega_{\rm prec} = \Theta/(2\Theta_{\rm rig})\ \Omega$, with $\Theta/\Theta_{\rm rig} = 1$ for the full MOI in a normal system, and $\Theta/\Theta_{\rm rig} < 1$ for a MOI that

is quenched because of the superfluid core.

The starting point of our experiments is an optically trapped, strongly interacting Fermi gas consisting of an equal mixture of ^{6}Li atoms in the lowest two atomic states [19, 20]. The broad 834-G Feshbach resonance [2] allows us to control the s-wave interaction. If not otherwise stated, the measurements presented here refer to the resonance center, where a unitarity-limited Fermi gas is realized [1, 2]. The cigar-shaped quantum gas is confined in a far red-detuned, single-beam optical dipole trap with additional axial magnetic confinement. The trap can be well approximated by a harmonic potential with radial oscillation frequencies $\omega_x = \omega_y \approx 2\pi \times 680\,\mathrm{Hz}$ and an axial frequency of $\omega_z = 2\pi \times 24\,\mathrm{Hz}$. The Fermi energy of the noninteracting gas is given by $E_F = \hbar(3N\omega_x\omega_y\omega_z)^{1/3}$, where $N = 6 \times 10^5$ is the total atom number. The Fermi temperature is $T_F = E_F/k = 1.3\,\mu\mathrm{K}$, with k denoting the Boltzmann constant.

Our scheme to study the rotational properties is described in detail in Ref. [17]. It is based on a rotating elliptical deformation of the trap, characterized by a small ellipticity parameter [17] $\epsilon' = 0.1$. In contrast to our previous work, we use a lower rotation frequency of $\Omega_{\mathrm{trap}} = 2\pi \times 200\,\mathrm{Hz} \approx 0.3\,\omega_x$. This low value allows us to avoid a resonant quadrupole mode excitation, which is known as an efficient mechanism for vortex nucleation [21, 22]. The excitation and detection of the precessing radial quadrupole mode also follows the procedures described in Ref. [17].

At this point it is important to discuss the consequences of residual trap imperfections, still present when we attempt to realize a cylindrically symmetric optical potential. As we showed in previous work [17], we can control the ellipticity down to a level of ∼1%. Moreover, deviations from perfect cylindrical symmetry may occur because of other residual effects, such as corrugations of the optical trapping potential. As a consequence, a certain rotational damping is unavoidable, but damping times can reach typically one second [17]. This has two main effects for our observations. First, our measurements yield precession frequencies slightly below Ω_{prec}. This is because of a delay time of 20 ms between turning off the rotating trap ellipticity and applying the surface mode excitation. It is introduced to make sure that any possible collective excitation resulting from the rotating trap has damped out when the mode precession is measured. Because of rotational damping during this delay time, the measured precession frequencies Ω'_{prec} are somewhat below Ω_{prec}. To compensate for this effect, we determine the corresponding damping parameter $\kappa = \Omega'_{\mathrm{prec}}/\Omega_{\mathrm{prec}}$ for each set of measurements, finding day-to-day variations with typical values between 0.85 and 0.9. The second effect is induced by friction with static (nonrotating) trap imperfections when the rotating ellipticity is applied. This leads to equilibrium values for Ω typically a few percent below Ω_{trap}. For this second effect there is no straightforward compensation, and it needs to be explicitly discussed when interpreting the experimental results.

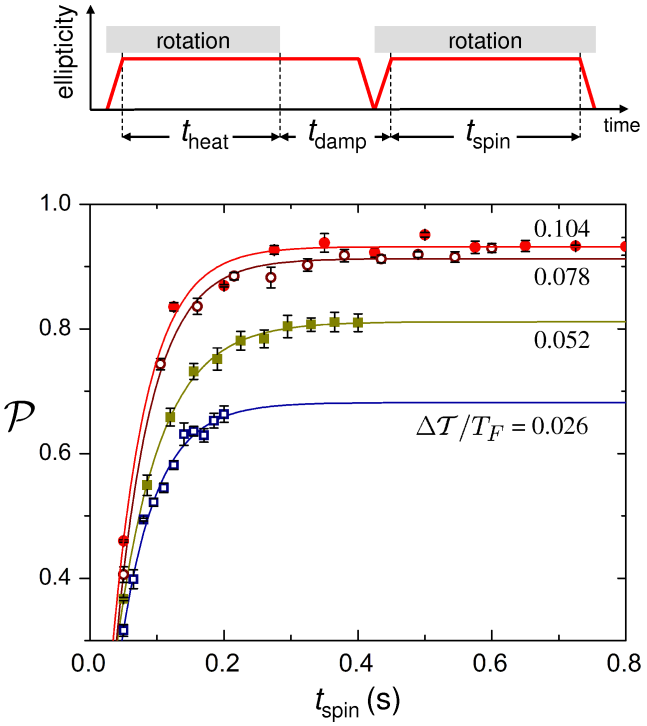

Figure 2: Precession parameter $\mathcal{P}$ versus spin-up time t_{spin} for various values of the final temperature, as characterized by the heating parameter $\Delta\mathcal{T}$ (see text). The quenching of the MOI shows up in the temperature-dependent saturation behavior. The applied timing sequence to facilitate measurements at constant temperature is illustrated above the graph. In these sets of measurements $\kappa = 0.85$.

Thermometry is performed after the whole experimental sequence. We damp out the rotation by stopping the trap rotation and keeping the ellipticity [23]. We convert the gas into a weakly interacting one by a slow magnetic field ramp to 1132 G, and we finally measure the temperature $\mathcal{T}$ [17]. Note that the isentropic conversion tends to decrease the temperature such that $\mathcal{T}$ is always somewhat below the temperature T at unitarity [24]. The relative statistical uncertainty of the temperature measurement is about 5% in the relevant temperature range.

For our further discussion, we introduce a dimensionless precession parameter $\mathcal{P}$ by normalizing our observable Ω_{prec} to its maximum possible value of $\Omega_{\mathrm{trap}}/2$,

$$\mathcal{P} = 2\,\frac{\Omega_{\mathrm{prec}}}{\Omega_{\mathrm{trap}}} = \frac{\Theta}{\Theta_{\mathrm{rig}}} \times \frac{\Omega}{\Omega_{\mathrm{trap}}}\,. \qquad (1)$$

Values $\mathcal{P} < 1$ show the presence of at least one of the two effects, namely the incomplete rotation of the normal part ($\Omega/\Omega_{\mathrm{trap}} < 1$) or the superfluid quenching of the MOI ($\Theta/\Theta_{\mathrm{rig}} < 1$). Our basic idea to distinguish between these two effects is based on the fact that $\Theta/\Theta_{\mathrm{rig}}$ rep-

resents a temperature-dependent equilibrium property, whereas $\Omega/\Omega_{\rm trap}$ reflects the spin-up dynamics. Therefore an increase of $\mathcal{P}$ observed at a fixed temperature can be attributed to the latter effect. This, however, is experimentally not straightforward because of the presence of residual heating. In the rotating trap we always observe some heating, which under all our experimental conditions can be well described by a constant rate $\alpha = 170\,\mathrm{nK/s} = 0.13\,T_F/\mathrm{s}$.

In a first set of experiments, to observe the spin-up dynamics at a fixed temperature, we apply a special procedure based on the timing scheme illustrated on top of Fig. 2. Our procedure takes advantage of the constant heating rate α to control the final temperature of the gas. We apply the trap rotation in two separate stages of duration $t_{\rm heat}$ and $t_{\rm spin}$. In an intermediate time interval of $t_{\rm damp} = 200\,\mathrm{ms}$ we damp out the rotation that is induced by the first stage [25]. The angular momentum disappears, but the heating effect remains [23]. The second stage spins the cloud up again and induces further heating. When $t_{\rm tot} = t_{\rm heat} + t_{\rm spin}$ is kept constant, we find that the total heating by the two rotation stages is $\Delta\mathcal{T} = \alpha\, t_{\rm tot}$. As only the second stage leads to a final angular momentum, $\mathcal{P}(t_{\rm spin})$ reveals the spin-up dynamics. A variation of the parameter $t_{\rm tot}$ controls $\Delta\mathcal{T}$ and thus allows for a variation of the final temperature $\mathcal{T} = \mathcal{T}_0 + \Delta\mathcal{T}$; the temperature offset $\mathcal{T}_0 \approx 0.11\,T_F$ is set by the initial cooling and some unavoidable heating during the experimental sequence without trap rotation.

Our experimental results for $\mathcal{P}(t_{\rm spin})$ are shown in Fig. 2 for four different values of the heating parameter $\Delta\mathcal{T}/T_F$ in a range between 0.026 to 0.104. This corresponds to a temperature range between about 0.14 and $0.21\,T_F$, where we expect the superfluid phase transition to occur. All four curves show qualitatively the same behavior. Within a few 100 ms, $\mathcal{P}$ rises before it saturates. It is straightforward to interpret this time-dependent increase of $\mathcal{P}$ in terms of the spin-up dynamics. The observed behavior can be well fit by simple exponential curves (solid lines) approaching a steady-state value. This fit yields a time constant of ∼50 ms for all four curves and allows us to extract the different saturation values for $\mathcal{P}$. Note that a characteristic spin-up time of about 50 ms is consistent with theoretical predictions for a collisionally hydrodynamic gas [17, 26].

The four curves in Fig. 2 clearly show a general temperature dependence of the saturation value of $\mathcal{P}$. For the two highest temperatures, however, both curves approach nearly the same saturation value of ∼0.95. This indicates that a superfluid core is very small or absent and that in both cases the hydrodynamic cloud rotates with an angular velocity Ω near the maximum possible value of $\Omega_{\rm trap}/2$. For the lower two temperatures, however, the saturation value shows a clear temperature dependence. At $\Delta\mathcal{T}/T_F = 0.026$ and 0.052, we observe $\mathcal{P}$ to saturate at 0.68 and 0.81. Normalizing these values

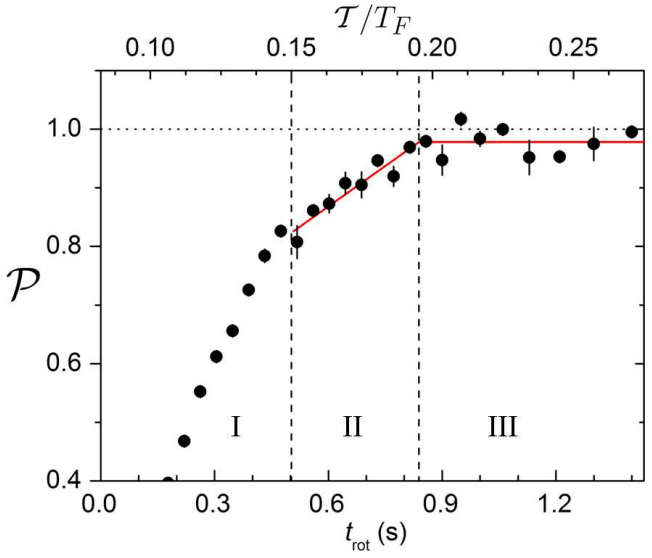

Figure 3: The precession parameter $\mathcal{P}$ as a function of the rotation time $t_{\rm rot}$ (lower scale); the upper scale shows the corresponding temperature $\mathcal{T}$. The vertical dashed lines separate the three different stages (I-III) discussed in the text. The second stage II corresponds to the case where the normal part is fully rotating and the MOI is quenched because of the presence of a superfluid core. For this measurement $\kappa = 0.90$.

to the maximum observed $\mathcal{P}$ at higher temperatures, we derive quenching factors for the MOI of $\Theta/\Theta_{\rm rig} = 0.73$ and 0.87, respectively.

Let us comment on the possible influence of vortices. We cannot exclude their presence, as their nucleation can proceed not only via a resonant quadrupole mode excitation [21, 22], but also via a coupling to the thermal cloud [27]. Vortices would result in additional angular momentum in the rotating cloud and its collective behavior would be closer to the normal case. This would tend to increase $\mathcal{P}$ at lower temperatures, and would counteract the behavior that we observe.

In a second set of experiments, we study the superfluid phase transition in a way which is experimentally simpler, but which requires the knowledge of the spin-up dynamics as obtained from the measurements presented before. Here the trap rotation is applied without any interruption and we observe the increase of $\mathcal{P}$ with the rotation time $t_{\rm rot}$; all other parameters and procedures are essentially the same as in the measurements before. In this procedure the temperature is not constant, but rises according to $\mathcal{T} = \mathcal{T}_0 + \alpha t_{\rm rot}$, where the heating rate $\alpha = 170\,\mathrm{nK/s}$ is the same as before and $\mathcal{T}_0 = 0.085 T_F$ is somewhat lower because of the less complex timing sequence.

Fig. 3 shows how $\mathcal{P}$ increases with the rotation time $t_{\rm rot}$; the upper scale shows the corresponding temperature $\mathcal{T}$. The observed increase in $\mathcal{P}$ generally results from both factors in Eq.(1), the rising $\Omega/\Omega_{\rm trap}$ and the

rising $\Theta/\Theta_{\rm rig}$. However, both effects contribute on different time scales, which allows us to distinguish between three different stages (I-III), as indicated in Fig. 3. For $t_{\rm rot} < 500\,{\rm ms}$ (stage I) the spin-up dynamics dominates and leads to a fast increase in $\mathcal{P}$. For intermediate times, $500\,{\rm ms} < t_{\rm rot} < 840\,{\rm ms}$ (stage II), $\mathcal{P}$ still increases, but at a much slower rate. Here, for a fully rotating normal part, the superfluid quenching of the MOI ($\Theta/\Theta_{\rm rig} < 1$) is the dominant effect. For $t_{\rm rot} > 840\,{\rm ms}$ (stage III), $\mathcal{P}$ saturates and acquires a value that is very close to the maximum, indicating the full rotation of a gas without any superfluid component.

For the superfluid phase transition, which occurs between stages II and III, we obtain a critical temperature of $\mathcal{T}_c/T_F = 0.195(15)$. The conversion of this value, measured in the weakly interacting regime, to the actual temperature in the unitarity limit yields values for T_c between $0.20\,T_F$ [28] and $0.24\,T_F$ [24]. This range for T_c is consistent with previous experimental results [4, 8, 29, 30] and theoretical predictions [1, 31].

The superfluid quenching effect in stage II can be quantitatively discussed in terms of the slope $s = \Delta(\Theta/\Theta_{\rm rig})/\Delta\mathcal{T}$ near the phase transition. Our data in Fig. 3 show an increase of the MOI according to $s = 4.2(5)\,T_F^{-1}$. This is fully consistent with the observed temperature dependence of the MOI in Fig. 2, from which we obtain $s = 3.5(4)\,T_F^{-1}$. In terms of the critical temperature T_c this slope corresponds to $s \approx 1.0\,T_c^{-1}$. We can compare this behavior with available predictions for the limits of BEC and BCS theory. For a BEC, the superfluid quenching effect is very small [32]. For a BCS-type system, Refs. [33, 34] predict a slope of $\sim 2.0\,T_c^{-1}$. Our observed behavior thus lies in between the two extremes of BEC and BCS.

In conclusion, we have demonstrated the quenching of the moment of inertia that occurs as a consequence of superfluidity in a strongly interacting Fermi gas. This effect provides us with a novel probe for the system as, in contrast to other common methods such as expansion measurements and studies of collective modes, it allows us to distinguish between the two possible origins of hydrodynamic behavior, namely collisions in a normal phase and superfluidity.

We thank L. Sidorenkov for discussions. We acknowledge support by the Austrian Science Fund (FWF) within SFB 15 (project part 21) and SFB 40 (project part 4).

* Present address: Institut für Quantensensorik, Universität Ulm, Germany

[1] S. Giorgini, L. P. Pitaevskii, and S. Stringari, Rev. Mod. Phys. **80**, 1215 (2008).
[2] M. Inguscio, W. Ketterle, and C. Salomon, eds., *Ultracold Fermi Gases* (IOS Press, Amsterdam, 2008), Proceedings of the International School of Physics "Enrico Fermi", Course CLXIV, Varenna, 20-30 June 2006.
[3] K. M. O'Hara *et al.*, Science **298**, 2179 (2002).
[4] C. A. Regal, M. Greiner, and D. S. Jin, Phys. Rev. Lett. **92**, 040403 (2004).
[5] J. Kinast *et al.*, Phys. Rev. Lett. **92**, 150402 (2004).
[6] M. Bartenstein *et al.*, Phys. Rev. Lett. **92**, 203201 (2004).
[7] C. Chin *et al.*, Science **305**, 1128 (2004).
[8] J. Kinast *et al.*, Science **307**, 1296 (2005).
[9] M. W. Zwierlein *et al.*, Nature **435**, 1047 (2005).
[10] P. Ring and P. Schuck, *The Nuclear Many Body Problem* (Springer, Berlin, 1980).
[11] G. B. Hess and W. M. Fairbank, Phys. Rev. Lett. **19**, 216 (1967).
[12] E. Kim and M. H. W. Chan, Science **305**, 1941 (2004).
[13] B. Clancy, L. Luo, and J. E. Thomas, Phys. Rev. Lett. **99**, 140401 (2007).
[14] F. Chevy, K. M. Madison, and J. Dalibard, Phys. Rev. Lett. **85**, 2223 (2000).
[15] P. C. Haljan, B. P. Anderson, I. Coddington, and E. A. Cornell, Phys. Rev. Lett. **86**, 2922 (2001).
[16] A. E. Leanhardt *et al.*, Phys. Rev. Lett. **89**, 190403 (2002).
[17] S. Riedl *et al.*, Phys. Rev. A **79**, 053628 (2009).
[18] F. Zambelli and S. Stringari, Phys. Rev. Lett. **81**, 1754 (1998).
[19] S. Jochim *et al.*, Science **302**, 2101 (2003).
[20] A. Altmeyer *et al.*, Phys. Rev. A **76**, 033610 (2007).
[21] K. W. Madison, F. Chevy, V. Bretin, and J. Dalibard, Phys. Rev. Lett. **86**, 4443 (2001).
[22] E. Hodby *et al.*, Phys. Rev. Lett. **88**, 010405 (2002).
[23] The temperature increase resulting from conversion of rotational energy into heat is neglibly small.
[24] Q. Chen, J. Stajic, and K. Levin, Phys. Rev. Lett. **95**, 260405 (2005).
[25] The ellipticity is kept at its full level while the rotation is turned off. To speed up the damping we increase the magnetic field to 920G.
[26] D. Guèry-Odelin, Phys. Rev. A **62**, 033607 (2000).
[27] P. C. Haljan, I. Coddington, P. Engels, and E. A. Cornell, Phys. Rev. Lett. **87**, 210403 (2001).
[28] L. Luo and J. E. Thomas, J. Low Temp. Phys. **154**, 1 (2009).
[29] L. Luo *et al.*, Phys. Rev. Lett. **98**, 080402 (2007).
[30] Y. Inada *et al.*, Phys. Rev. Lett. **101**, 180406 (2008).
[31] R. Haussmann and W. Zwerger, Phys. Rev. A **78**, 063602 (2008).
[32] S. Stringari, Phys. Rev. Lett. **76**, 1405 (1996).
[33] M. Farine, P. Schuck, and X. Viñas, Phys. Rev. A **62**, 013608 (2000).
[34] M. Urban and P. Schuck, Phys. Rev. A **67**, 033611 (2003).